

Film growth of ^4He adsorbed in mesopores

Hiroki Ikegami,* Tomohisa Okuno, Yoji Yamato, Junko Taniguchi,† and Nobuo Wada‡
Institute of Physics, Basic Science, Graduate School of Arts and Sciences, University of Tokyo,
Komaba 3-8-1, Meguro-ku, Tokyo 153-8902, Japan

Shinji Inagaki and Yoshiaki Fukushima
Toyota Central R&D Laboratories, Inc., Yokomichi, Nagakute, Aichi 480-1192, Japan
 (Received 16 June 2003; published 2 September 2003)

The film growth of ^4He adsorbed in mesoporous substrates was investigated by accurate vapor pressure measurements for various pore sizes between 18 Å and 47 Å. The ^4He film adsorbed on the pore wall forms a cylindrical tube, but does not show the capillary condensation. Completion of the first layer and the full pore coverage could be identified for all pore sizes studied. In the first layer, no pore size dependence of the film growth was found, indicating that the growth of this layer was dominated primarily by the van der Waals force from the substrate. Film growth after the first layer completion, however, has a strong pore size dependence. The ratio of the first layer completion and the full pore coverage agrees well with that expected from the pore dimensions.

DOI: 10.1103/PhysRevB.68.092501

PACS number(s): 67.40.-w, 67.70.+n

One of the central themes of condensed-matter physics is the quantum fluid in reduced dimensionality. Helium 4 and 3 in one-dimensional (1D) or quasi-one-dimensional systems have recently received much attention since the realization of such systems has become possible in the laboratory. Helium film adsorbed within mesoporous materials¹⁻³ or carbon nanotubes^{4,5} is a good candidate to realize these systems. Our previous experiments showed that the second layer of the ^4He film adsorbed in 18-Å mesoporous substrate, which forms a cylindrical fluid tube on the pore wall, has a temperature linear heat capacity below 0.3 K.^{1,6} This heat capacity is explained by the 1D phonon excitation with a wave vector parallel to the pore axis.

^4He film adsorbed in pores with a diameter d larger than 50 Å, in contrast, shows a superfluid transition through the system size dependent Kosterlitz-Thouless (KT) transition.⁷ In such pore sizes, the unbinding of a vortex pair separated less than $\pi d/2$ destroys the phase coherence and determines the transition temperature.⁸ However, this vortex mechanism will break down for pores with a diameter comparable to the vortex core size, which is experimentally estimated to be 25 ± 12 Å.⁷ Therefore, the pore size is crucial in the superfluid transition. Between 18 Å and 50 Å the nature of the ^4He film is expected to show the crossover from 2D to 1D.

The mesoporous substrate FSM (Refs. 9,10) is a suitable material for study of the crossover from 1D to 2D. FSM is a family of highly ordered mesoporous silica crystals with a regular arrangement of uniform hexagonal channels. The pore size is uniform and can be precisely controlled between 10 Å and 50 Å using alkyltrimethylammonium ions [$\text{C}_n\text{H}_{2n+1}\text{N}^+(\text{CH}_3)_3$] of different alkylchain length in the synthesizing process of this material. These features make it possible for us to investigate the influence of pore size on ^4He film, yet little is known about the behavior of the film adsorbed in this substrate.

In this paper, we report the film growth of ^4He adsorbed in mesoporous substrates with a pore diameter ranging from 18 to 47 Å investigated by precise vapor pressure measure-

ments. This measurement is an excellent means of studying film growth, because from it can be deduced the chemical potential μ_a of the adsorbed phase and, in principle, the complete thermodynamic properties can be understood.

The FSM substrates used in this work have pores 18, 22, 28, and 47 Å in diameter. The three smaller pores correspond to $n=10$, 14, and 16, respectively, and the 47-Å pore is enlarged one from $n=16$ by the addition of mesitylene.¹¹ These substrates are in powder form with a particle size of about 0.3 μm . They were mixed with 60 μm of silver powder in a 2:1 weight ratio and pressed onto the body of a copper or silver sample cell for good thermal contact. After being dehydrated in a vacuum at 200 °C, the cell was sealed in a ^4He atmosphere. Surface area S was determined by the Brunauer-Emmett-Teller (BET) fitting of an N_2 adsorption isotherm at 77 K. The obtained surface areas are summarized in Table I. The area of FSM grains, as estimated from the powder size, is less than 1% of the total surface area. The vapor pressure P was measured using a capacitive strain gauge with a 125- μm -thick Kapton sheet as a diaphragm. On one side of the sheet a thin film of 100-nm-thick Au was sputtered, which constitutes one electrode of the capacitor. Another fixed electrode was placed 50 μm away from the diaphragm; the capacitance between them was about 4 pF. The pressure was calibrated against the ^4He saturated vapor pressure. Its sensitivity was 2×10^{-3} mbar. The diaphragm

TABLE I. Surface area obtained by the BET fitting of an N_2 adsorption isotherm at 77 K and the pressure range for fitting. n_1 determined from the compressibility minimum is also summarized.

	18 Å	22 Å	28 Å	47 Å
Surface area (m^2)	195	141	146	103
BET fitting region (P/P_0)	0.05–0.15	0.05–0.15	0.05–0.22	0.05–0.22
n_1 (mmol)	2.4	2.2	2.5	1.8

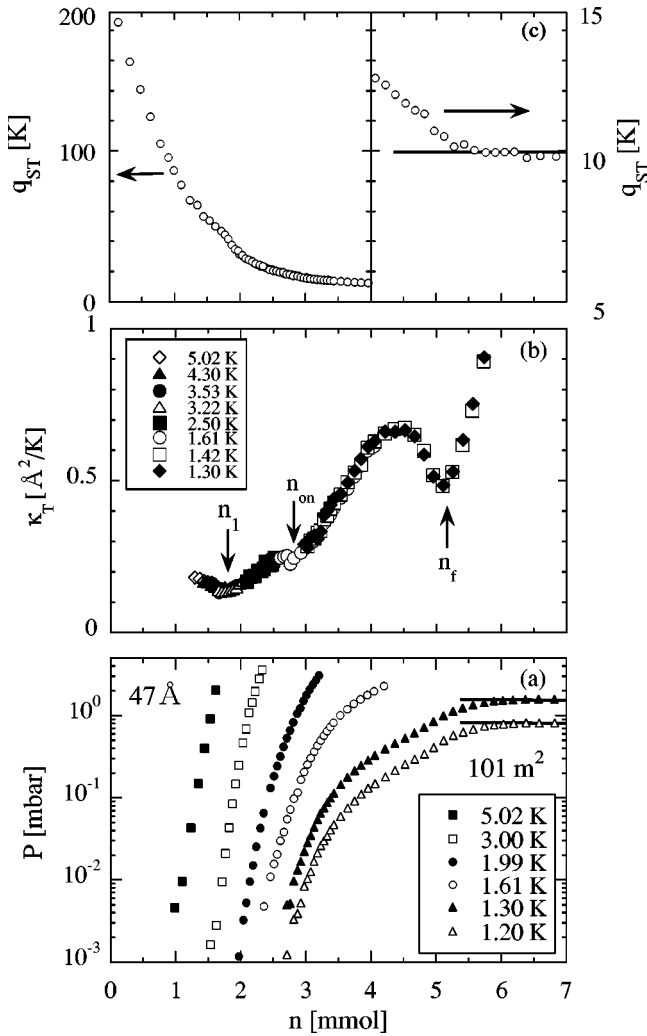


FIG. 1. (a) Typical vapor pressure isotherm for the ^4He films adsorbed in $47\text{-}\text{\AA}$ pores. Solid lines represent the saturated vapor pressure at corresponding temperature. The surface area is 103 m^2 , determined by the BET fitting of an N_2 vapor pressure isotherm. (b) Two-dimensional compressibility. (c) Isosteric heat of adsorption.

moved linearly with pressure below 4 mbar. The gauge and the cell were linked together through a capillary and mounted on the same stage of a ^3He refrigerator to avoid the thermomolecular effect. The ^4He sample was introduced and annealed at a temperature where the vapor pressure was around 1 mbar to ensure a uniform film.

The typical vapor pressure isotherms are shown in Fig. 1 (a) as a function of ^4He adsorbed amount n , with the results of the $47\text{-}\text{\AA}$ substrate shown as representative. At low- n region the vapor pressure is small compared to the saturated vapor pressure P_0 at corresponding temperature. With increasing n , P monotonically increases, finally reaching P_0 at the corresponding temperature. Note that no plateau associated with the capillary condensation was observed in the isotherms.

To understand how the film grows, we calculated the two-dimensional compressibility defined by

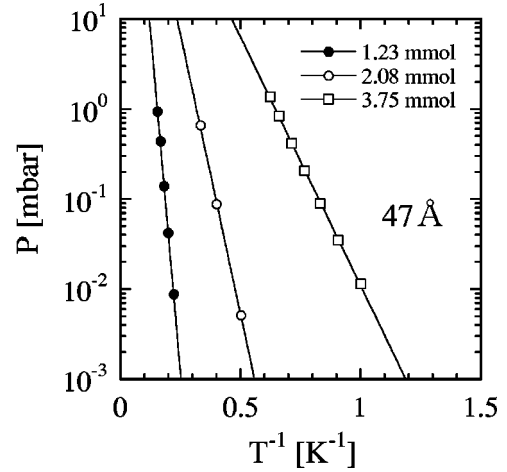


FIG. 2. Typical temperature dependence of ^4He vapor pressure adsorbed in $47\text{-}\text{\AA}$ pores.

$$\kappa_T = \frac{S}{n^2} \left[\frac{\partial \mu_a}{\partial n} \right]^{-1} = \frac{S}{n^2 k_B T} \frac{\partial n}{\partial \ln P}, \quad (1)$$

where S is the surface area, k_B is the Boltzmann constant, and T is the temperature. The second part of Eq. (1) applies if the gas is treated as ideal. The obtained κ_T is shown in Fig. 1(b). With increasing n , κ_T evolves in a very interesting way. Below 1.8 mmol it decreases with increase of n , indicating that the film becomes hard due to the increase in areal density. Then it shows a minimum at n_1 . This minimum is believed to be a second-layer promotion similar to the case of ^4He adsorbed on graphite.^{12,13} After the second-layer promotion, κ_T gradually increases and shows a small but reproducible substep at n_{on} . Our preliminary studies with a torsional oscillator found that n_{on} is an onset coverage of the superfluid transition.¹⁴ With further increasing n , κ_T shows another large minimum at n_f .

The temperature dependence of P gives us another thermodynamic information about the film. As seen in Fig. 2, the isosteric heat of adsorption q_{ST} defined by $q_{ST} = -\partial \ln P / \partial (1/T)$ is independent of temperature in the pressure range between 10^{-3} mbar and 1 mbar. q_{ST} obtained by fitting is summarized in Fig. 1(c). Note that q_{ST} is not for a fixed temperature, since the fittings were performed between 10^{-3} mbar and 1 mbar, and thus the temperature range changes greatly with coverage. It is typically 2.5–4.0 K at n_1 and 0.90–1.4 K at n_f .

At n_1 , q_{ST} shows a small substep and is about 40 K, a value similar to that of ^4He adsorbed on graphite.¹⁵ In addition, the areal density at n_1 deduced from the surface area obtained by the N_2 vapor pressure isotherm is 10.7 nm^{-2} ; this value is also consistent with the density of the second-layer promotion in the case of graphite substrate.¹⁵ These facts strongly support the conclusion that the minimum in κ_T at n_1 corresponds to the second layer promotion.

Just after n_f , q_{ST} shows a constant value of 10 K, a value which exactly corresponds to that of the bulk ^4He liquid.¹⁶ This fact implies that ^4He atoms fill the pores completely

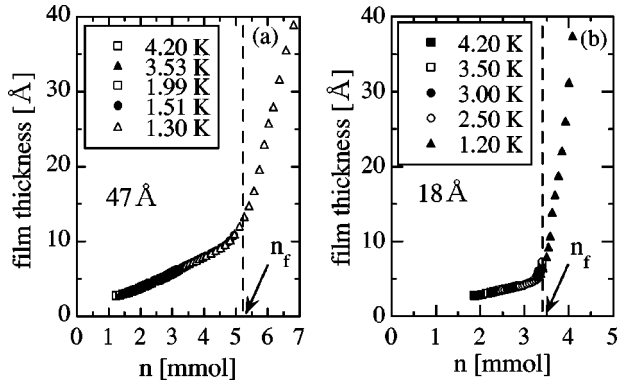


FIG. 3. Film thickness of ^4He adsorbed on the surface of the FSM grains obtained using the Frenkel-Halsey-Hill model [(a) 47 Å, (b) 18 Å].

above n_f . To more clearly see the behavior around n_f , we calculated the thickness δ of the film adsorbed *on the surface of the FSM grains* from the experimental data using the Frenkel-Halsey-Hill (FHH) model.¹⁷ (Note that δ is not the thickness of the film inside the pore.) In this model, structureless ^4He fluid film formed on a flat surface with a chemical potential of $-\gamma/\delta^3$ measured from bulk liquid is assumed to coexist with ^4He vapor, where γ is the adsorption coefficient. Consequently, the film thickness is given by $\delta = [T/\gamma \ln(P_0/P)]^{-1/3}$. In our case, the introduced ^4He atoms are mainly adsorbed inside pores, but a small amount is adsorbed on the surface of the grains. While the film on the grains has the same chemical potential as that inside the pore, the thickness of the both films is not same. Because the size of the FSM grain is about $0.3 \mu\text{m}$, the surface of the grain is considered as an approximately planar surface. Therefore, δ obtained by the FHH model can be regarded as the thickness of the film on the grains. The obtained δ for the 47-Å pore is shown in Fig. 3(a), where we used $\gamma = 1100 \text{ K Å}^3$, the value for a glass substrate.¹⁷ δ increases in proportion to n below n_f , thereafter showing a steep increase. This behavior can be understood as follows. At n_f the pores are completely filled with ^4He , resulting in sudden reduction of the surface area for adsorption. After n_f , the introduced ^4He atoms are mainly adsorbed on the grain surface. This causes the steep increase in δ after n_f . The slope of δ after n_f is eight times steeper than before n_f . This indicates that, assuming that the surface area of the grains is 1% of the total surface area, ^4He atoms are adsorbed into the pores and onto the surface of the grains in a 12:1 ratio, resulting in the gradual compression of ^4He in the pores.

^4He vapor pressure results with other diameter substrates have similar features to those with the 47-Å substrate. In Fig. 4 the compressibility obtained with all substrates are shown as a function of n/n_1 . For all substrates we found two distinct minima, which are considered to be the second-layer promotion (n_1) and the full pore (n_f), for the same reasons as described for the 47-Å substrate. On the other hand, a small substep n_{on} is found only with the 28-Å and 47-Å substrates.

It is important to mention that any signatures of the capillary condensation are not observed for any substrates. The

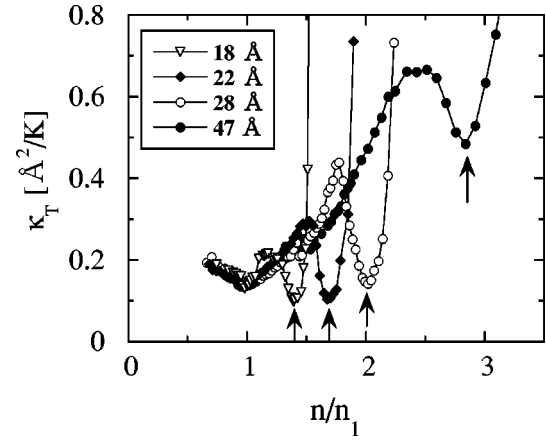


FIG. 4. Compressibility of various pore sizes as a function of n/n_1 . Arrows indicate the full pore coverage n_f .

absence of the capillary condensation may be related to some facts; the small size of pores, large zero-point motion, the strong substrate potential, and heterogeneity of the substrate. Though some theoretical investigations for pores with several angstroms of diameter exist,^{18–20} none of them can be directly applied for our system. Further studies, such as path-integral Monte Carlo calculations with parameters of our system, are eagerly desired.

Below n_1 , κ_T and q_{ST} (not shown) of all substrates show the same n/n_1 dependence, indicating that ^4He film growth is dominated primarily by the potential from the substrates and the pore size difference has little effect. On the other hand, a clear difference is observed above n_1 . For smaller pores, a smaller amount of ^4He is enough to fill the pore completely. The ratio n_f/n_1 for all pore sizes is summarized in Table II. Here we also show the ratio of the cross-section area (S_f/S_1) obtained with a simple calculation that $S_f = \pi(d/2)^2$ is the cross section area of a pore with a diameter d and $S_1 = S_f - \pi(d/2 - 3.58 \text{ Å})^2$ is that of the cylindrical shell of the first layer with a thickness of 3.58 Å, the value which is a monolayer thickness of the bulk liquid density at saturated vapor pressure. S_f/S_1 is about 10% larger than n_f/n_1 , which is reasonable because the density of the first few layers is expected to be larger than that of the bulk liquid.

The film thickness with the 18-Å pore obtained within the FHH model is shown in Fig. 3(b). At n_f , δ abruptly begins to increase due to the sudden reduction of the surface area for adsorption, which is caused by complete ^4He filling of the pores. The slope of δ after n_f is 37 times steeper than before n_f . This suggests that, compared with the 47-Å pores,

TABLE II. Pore size dependence of n_{on}/n_1 and n_f/n_1 determined by the vapor pressure results. Calculated cross-section area ratio S_f/S_1 is also shown (see text).

	18 Å	22 Å	28 Å	47 Å
n_{on}/n_1			1.4	1.5
n_f/n_1	1.4	1.7	2.0	2.9
S_f/S_1	1.57	1.83	2.24	3.55

the proportion of the ^4He atoms entering the pores is small. This is reasonable since for a larger pore, ^4He in the pore is more compressed, and thus a great number of ^4He atoms can enter the pores.

Between n_1 and n_f , δ increases almost linearly and the rate of increase is consistent with that expected from the surface area inside the pores, suggesting that the ^4He film is formed on the pore wall. In this region, in the 18-Å pore, the heat capacity of the second-layer film is proportional to the temperature below 0.3 K.¹ This heat capacity is explained by the 1D phonon excitation with a wave vector parallel to the pore axis. The phonon velocity obtained from the heat-capacity data agrees well with that obtained from our previous vapor pressure measurement,⁶ and the agreement strongly suggests that the cylindrical ^4He tube on the pore wall has a 1D property.

Inside the 47-Å pore, on the other hand, the superfluid was observed above n_{on} by the torsional oscillator.¹⁴ In this experiment a large superfluid decoupling of 7.2% was found, indicating that the film in the pore is certainly superfluid since the decoupling due to the film adsorbed on the FSM grains is 1% at most. The temperature dependence of the superfluid density below the transition temperature is not as sharp as expected by the KT transition. This is explained by the system size dependent KT theory, where the vortex

unbinding mechanism plays a significant role just as the 2D system. The crossover from 2D to 1D is expected between 18-Å and 47-Å pore size. Our results on film growth will be helpful in interpreting further torsional oscillator and heat-capacity experiments in this pore size range.

In conclusion, we investigated the film growth of ^4He adsorbed in mesoporous substrates by accurate vapor pressure measurements for various pore sizes between 18 Å and 47 Å. The ^4He film adsorbed on the pore wall forms a cylindrical tube, but does not display the capillary condensation. The first-layer completion and the full pore coverage could be identified for all pore sizes studied. In the first layer, no pore size dependence of the film growth was found, indicating that the growth of this layer was mainly dominated by the van der Waals force from the substrate. The film growth after the first-layer completion, however, had a strong pore size dependence. The pore size dependence of n_f/n_1 showed good agreement with that expected from the pore dimensions. These data provide us with helpful information for future study of the nature of the Bose fluid and the superfluid transition of the ^4He film adsorbed in mesoporous substrates.

The authors thank M. H. W. Chan for stimulating discussions. This work was partly supported by a Grant-in-Aid for Scientific Research from the Ministry of Education, Culture, Sports, Science and Technology, Japan.

*Present address: Low Temperature Physics Laboratory, RIKEN (The Institute of Physical and Chemical Research), Hirosawa 2-1, Wako, Saitama, 351-0198, Japan. Electronic address: hikegami@postman.riken.go.jp

†Present address: Institute for Solid State Physics, University of Tokyo, 5-1-5 Kashiwanoha, Kashiwa, Chiba 277-8581, Japan.

‡Present address: Department of Physics, Graduate School of Science, Nagoya University, Chikusa-ku, Nagoya, 464-8602, Japan.

¹N. Wada, J. Taniguchi, H. Ikegami, S. Inagaki, and Y. Fukushima, Phys. Rev. Lett. **86**, 4322 (2001).

²J. Taniguchi, T. Okuno, H. Ikegami, and N. Wada, J. Low Temp. Phys. **126**, 259 (2002).

³M.W. Cole and E.S. Hernández, Phys. Rev. B **65**, 092501 (2002).

⁴W. Teizer, R.B. Hallock, E. Dujardin, and T.W. Ebbesen, Phys. Rev. Lett. **82**, 5305 (1999).

⁵M.C. Gordillo, J. Boronat, and J. Casulleras, Phys. Rev. B **61**, R878 (2000).

⁶J. Taniguchi, H. Ikegami, and N. Wada, Physica B **329-333**, 274 (2003).

⁷K. Shirahama, M. Kubota, S. Ogawa, N. Wada, and T. Watanabe, Phys. Rev. Lett. **64**, 1541 (1990).

⁸T. Minoguchi and Y. Nagaoka, Prog. Theor. Phys. **80**, 397 (1988).

⁹S. Inagaki, A. Koiwai, N. Suzuki, Y. Fukushima, and K. Kuroda, Bull. Chem. Soc. Jpn. **69**, 1449 (1996).

¹⁰S. Inagaki, Y. Fukushima, and K. Kuroda, J. Chem. Soc., Chem. Commun. **22**, 680 (1993).

¹¹S. Inagaki, Y. Yamada, Y. Fukushima, and K. Kuroda, Stud. Surf. Sci. Catal. **92**, 143 (1994).

¹²G. Zimmerli, G. Mistura, and M.H.W. Chan, Phys. Rev. Lett. **68**, 60 (1992).

¹³P.A. Crowell and J.D. Reppy, Phys. Rev. B **53**, 2701 (1996).

¹⁴Y. Yamato, H. Ikegami, T. Okuno, J. Taniguchi, and N. Wada, Physica B **329-333**, 284 (2003).

¹⁵D.S. Greywall and P.A. Busch, Phys. Rev. Lett. **67**, 3535 (1991).

¹⁶Fitting of the temperature dependence of saturated vapor pressure at around 1 K gives $q_{ST} = 10$ K.

¹⁷E. Cheng and M.W. Cole, Phys. Rev. B **38**, 987 (1988).

¹⁸R.A. Trasca, M.M. Calbi, and M.W. Cole, Phys. Rev. E **65**, 061607 (2002).

¹⁹C. Gu and G.H. Gao, Phys. Chem. Chem. Phys. **4**, 4700 (2002).

²⁰M.M. Calbi, F. Toigo, S.M. Gatica, and M.W. Cole, Phys. Rev. B **60**, 14 935 (1999).